Experimental active structural acoustic control of simply supported plates using a weighted sum of spatial gradients

Daniel R. Hendricks and William R. Johnson
Department of Mechanical Engineering, Brigham Young University, Provo, Utah 84602

Scott D. Sommerfeldt
Department of Physics and Astronomy, Brigham Young University, Provo, Utah 84602

Jonathan D. Blotter[a)]
Department of Mechanical Engineering, Brigham Young University, Provo, Utah 84602

(Received 17 March 2014; revised 18 August 2014; accepted 30 September 2014)

A limitation currently facing active structural acoustic control (ASAC) researchers is that an ideal minimization quantity for use in the control algorithms has not been developed. A novel parameter termed the "weighted sum of spatial gradients" (WSSG) was recently developed for use in ASAC and shown to effectively attenuate acoustic radiation from a vibrating flat simply supported plate in computer simulations. This paper extends this research from computer simulations and provides experimental test results. The results presented show that WSSG is a viable control quantity and provides better results than the volume velocity approach. The paper also investigates several of the challenges presented by the use of WSSG. These include determining a method to measure WSSG experimentally, an analysis of the influence of noise on WSSG control results and complications presented when degenerate modes exist. Results are shown and discussed for several experimental configurations. © *2014 Acoustical Society of America*. [http://dx.doi.org/10.1121/1.4898046]

PACS number(s): 43.50.Ki [LC] Pages: 2598–2608

I. INTRODUCTION

One of the main limitations facing active structural acoustic control (ASAC) researchers is that a suitable parameter has not yet been discovered which can be easily implemented as the minimization quantity in the control algorithms. Several parameters have been attempted but most have been shown to be somewhat impractical or cumbersome to use. These include simply minimizing the vibration at a single point,[1,2] minimizing volume velocity,[3–5] and minimizing acoustic properties such as far field sound pressure and total radiated sound power.[6,7]

Recently, a new parameter was developed by Fisher *et al.*[8] which showed significant potential as a minimization quantity which could attenuate sound levels with relatively easy implementation. This parameter consists of the weighted sum of the squared displacement field, w, and the squared spatial derivatives, $\partial w/\partial x$, $\partial w/\partial y$, and $\partial^2 w/\partial x \partial y$. Fisher *et al.* initially termed the quantity "V_{Comp}" (for composite velocity) since the preliminary equations were based off the spatial derivatives of the velocity field. This name has been changed to the weighted sum of spatial gradients (WSSG) to more accurately describe the quantity. Fisher *et al.* used computer simulations to show sound attenuation could be achieved by minimizing WSSG at any point on the plate by applying a single point force to the plate. The simulated results provided equal or better attenuation levels than minimizing either volume velocity or structural intensity for a simply supported plate. It was also shown that WSSG had a significant advantage because it required a closely spaced, four accelerometer array treated like a single sensor placed on the surface of the plate. This is in contrast to the arrays of sensors spread either across the face of the plate or in the radiated sound field required by the other techniques. Furthermore, no information about the type or location of the disturbance force is needed. The work by Fisher *et al.* showed through computer simulations that the terms in the WSSG minimization quantity have local characteristics that have some relation to the global acoustic radiation modes and that minimizing WSSG generally has a similar effect as reducing the acoustic radiation modes.

This paper builds on the research of Fisher *et al.* and experimentally applies the WSSG technique to flat rectangular simply supported plates. In this paper, a brief overview of the WSSG theory will be provided, followed by additional computer simulations and analyses which were made necessary by advances in the experimental research. The experimental WSSG control results are then presented and discussed. It is shown that WSSG control provides a viable option for use in attenuating noise from vibrating flat rectangular simply supported plates.

II. OVERVIEW OF THE WSSG THEORY

This section provides a brief overview of the WSSG control approach. A more complete derivation is presented by Fisher *et al.*[8]

The idea for WSSG came about when researchers began looking for a structural quantity that is uniform across the entire measurement surface. The hypothesis was that a spatially uniform quantity would provide a significant advantage over other ASAC parameters because it would largely eliminate the sensitivity of the performance on the error

[a)]Author to whom correspondence should be addressed. Electronic mail: jblotter@byu.edu

sensor location and would not require *a priori* knowledge of the structure. The need for multiple error sensors, selecting error sensor locations, and knowledge about the vibration of the structure are three major drawbacks to current ASAC techniques which it was hypothesized the WSSG approach would overcome.

It was noted by Fisher *et al.*[8] that the four quantities w, and the spatial derivatives $\partial w/\partial x$, $\partial w/\partial y$, and $\partial^2 w/\partial x \partial y$ each target different locations on a vibrating simply supported plate. They discovered that a near spatially uniform value can be calculated if each term is multiplied by a scaling factor and then all four terms summed together. WSSG was thus defined as the summation of these four terms, each multiplied by a weighting value (α, β, γ, δ) as shown in Eq. (1) by

$$\mathrm{WSSG} = \alpha(w)^2 + \beta\left(\frac{\partial w}{\partial x}\right)^2 + \gamma\left(\frac{\partial w}{\partial y}\right)^2 + \delta\left(\frac{\partial^2 w}{\partial x \partial y}\right)^2. \tag{1}$$

While w represents the displacement in these terms, it should be noted that for time harmonic excitation sources, velocity or acceleration could equally be used. The only difference between using displacement and using either velocity or acceleration is that velocity and acceleration are scaled by the factors $i\omega$ and $(i\omega)^2$, respectively.

The scaling factors that make the WSSG field nearly uniform for a simply supported plate are related to the wave numbers and can be calculated for each resonance frequency as

$$\alpha = 1, \quad \beta = \left(\frac{L_x}{m\pi}\right)^2, \quad \gamma = \left(\frac{L_y}{n\pi}\right)^2, \quad \text{and} \quad \delta = \left(\frac{L_x L_y}{mn\pi^2}\right)^2, \tag{2}$$

where L_x and L_y are the lengths of the plate in the x and y directions, and m and n are the structural mode numbers corresponding to the frequency.

III. ANALYTICAL ANALYSIS AND SIMULATIONS

In order to create experimental control plots using WSSG as the minimization quantity it was first necessary to advance the analytical research which Fisher *et al.*[8] initiated. This additional research is broken into three sections; a further analysis of the weights, the determination of a method to measure the spatial derivatives, and an analysis of the effects of degenerate modes on WSSG.

A. A further analysis of the weights

As noted in Eqs. (2), the weights derived for use in WSSG are functions of the structural modes. These weighting functions work well if a plate is vibrating at a single resonance frequency because the calculated weights will give the desired uniform WSSG field across the face of the entire plate. However, if there are multiple resonance frequencies being excited, or if the frequency being excited is not near a resonance frequency, then Eqs. (2) have less applicability. Fisher *et al.*[8] recognized this, but to implement control over a range of resonances they chose to simply average the weights over the first 15 modes and use those values in the control algorithm. Using this method, they were able to use the same weights for a range of frequencies and they achieved reasonable success in controlling sound radiating from each of the resonance frequencies. However, further research was required to determine if this actually was the best method for calculating the weights.

In this work, several new methods for calculating weights were devised and tested using MATLAB based simulations. Each simulation modeled a simply supported plate being acted on by two point sources, one to excite the plate and the other to control it. Control was achieved by optimizing the phase and magnitude of the second force to drive WSSG to a minimum at a randomly selected point on the plate. The equations describing the vibration of the plate are given by

$$w(x,y) = \sum_{q=1}^{F} \frac{f_q}{\rho_s h} \sum_{m}^{\infty} \sum_{n}^{\infty} \frac{W_{mn}(x,y) W_{mn}(x_q,y_q)\left[\omega_{mn}^2 - \omega^2 - i\eta\omega_{mn}^2\right]}{\left[\omega_{mn}^2 - \omega^2\right]^2 + \eta^2 \omega_{mn}^4}, \tag{3}$$

$$W_{mn}(x,y) = \frac{2}{\sqrt{L_x L_y}} \sin\left(\frac{m\pi x}{L_x}\right) \sin\left(\frac{n\pi y}{L_y}\right), \tag{4}$$

$$\omega_{mn} = \sqrt{\frac{D}{\rho_s h}\left(\frac{m^2\pi^2}{L_x^2} + \frac{n^2\pi^2}{L_y^2}\right)}, \tag{5}$$

$$D = \frac{Eh^3}{12(1-\nu^2)}, \tag{6}$$

where f_q is the amplitude of the qth driving force (primary or control), ρ_s is the density of the plate, E is Young's modulus, ν is Poisson's ratio, h is the thickness of the plate, and L_x and L_y are the x and y dimensions of the plate, respectively. WSSG was calculated using the displacement and the derivatives $\partial w/\partial x$, $\partial w/\partial y$, and $\partial^2 w/\partial x \partial y$. To determine effectiveness, the sound power emitted from the plate was calculated with the controller toggled on and off using the method of elementary radiators.[9]

It was determined that the two methods for calculating the weights which provided the most overall attenuation were using an average (mean) value calculated over the modes of interest, and adapting the weights so that the controller used the weights of the nearest resonance frequency. When these simulations were plotted on the same graph (see Fig. 1), it became apparent that there was little difference

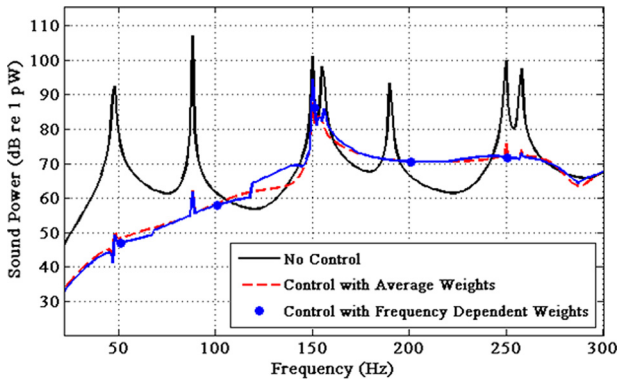

FIG. 1. (Color online) Simulated radiated power for two methods of calculating the WSSG weights.

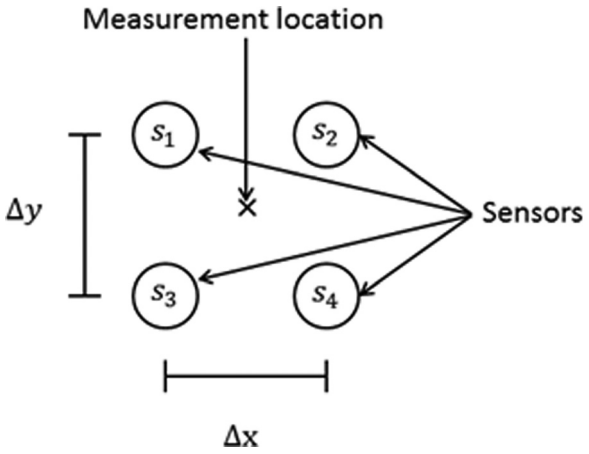

FIG. 2. Schematic of accelerometer spacing used to measure WSSG.

between the two methods. This implies that the weights used in WSSG are fairly robust and knowing the exact values of the weights is not needed. It was determined that getting the correct order of magnitude of the weights is important but getting the exact number is less so.

This information indicates that small gains could possibly be made using different methods to obtain the weights but the gains would be minimal. Therefore, further research on the method of calculating the exact optimum values of the WSSG weights was not pursued. For the remainder of this work, an average of the weights over the range of interest was used in all tests. This means a single value was calculated for the weights (α, β, γ, δ) and hard coded into the controller for each configuration. Doing this means that the uniform nature of WSSG across the plate is diminished slightly because the weights are not optimized for each frequency, but its ability to minimize sound radiation from the plate does not suffer significantly.

B. Measuring the spatial derivatives

In order to use WSSG on an experimental plate, a method needed to be devised to measure the four terms used in the summation; w, $\partial w/\partial x$, $\partial w/\partial y$, and $\partial^2 w/\partial x \partial y$. As was noted in Sec. II, w represents the transverse displacement, but for time harmonic excitation sources the transverse velocity or acceleration could also be used. Many methods, including strain gauges,[10] lasers, and shaped polyvinylidene fluoride films,[11] were explored to measure these derivatives. The best solution based on both accuracy and ease of implementation was determined to be an array of four closely spaced accelerometers. The signals from these accelerometers were then combined to form numerical approximations of the derivative terms using the centered difference approximation of the first derivative. A schematic of the experimental setup is shown in Fig. 2, with the corresponding WSSG terms given in Eqs. (7)–(10)

$$w \approx \frac{s_1 + s_2 + s_3 + s_4}{4}, \tag{7}$$

$$\frac{\partial w}{\partial x} \approx \frac{s_2 - s_1 + s_4 - s_3}{2\Delta x}, \tag{8}$$

$$\frac{\partial w}{\partial y} \approx \frac{s_1 - s_3 + s_2 - s_4}{2\Delta y}, \tag{9}$$

$$\frac{\partial^2 w}{\partial x \partial y} \approx \frac{s_2 - s_1 + s_3 - s_4}{\Delta x \Delta y}. \tag{10}$$

Each sensor s_i represents the instantaneous acceleration coming from each accelerometer, and Δx and Δy represent the x and y distance between the accelerometers, respectively. Chapra and Canale[12] note that these equations are approximations derived from the Taylor series expansion and contain truncation error. The central difference method has a truncation error on the order of (Δx^2) which means the larger the distance between the sensors, the more truncation error will exist. This indicates the accelerometers should be placed close to each other to minimize the effects from truncation error.

However, truncation error is not the only source of error in the setup; the noise levels within the signals must also be taken into consideration. Generally, random noise can cause a significant problem if the noise levels are within a few orders of magnitude of the measurements. However, because several of the WSSG terms are formed by subtracting half of the readings from each other, the random noise could actually have a significant effect if it is within a few orders of magnitude of the *difference* between two readings. Two closely spaced accelerometers will read similar magnitudes and so ideally should be placed further apart in order to increase the probability that the two accelerometers will read significantly different values. This will minimize the effects of noise in the measurements.

The optimal distance between the accelerometers is thus influenced by two opposing influences. Finite differencing has less truncation error when the measurement points are closer, but measurement noise is less of a factor when the measurement points are farther apart. These opposing influences necessitated the creation of an optimization routine in order to determine the best spacing of the accelerometers based on the expected noise levels.

A simulation was designed to calculate WSSG on a flat plate using the finite difference method rather than taking analytical derivatives. This simulation calculated the transverse accelerations at a grid of points on a plate and then used Eqs. (7)–(10) to estimate the displacement and three spatial derivatives at the center of the four points. WSSG was then calculated from these finite difference derivative terms and the

finite difference WSSG ($WSSG_{FD}$) was compared to the analytical WSSG ($WSSG_A$) calculated from the previous simulations. In order to simulate actual accelerometer readings, random noise was added to the transverse accelerations at each point in the $WSSG_{FD}$. The magnitude of this random noise was directly correlated to the measured random noise levels in the actual accelerometers used to run the tests. This was done by measuring the signal-to-noise ratio of the actual data and then adding random noise to the simulation using the MATLAB randn function until the same signal-to-noise ratio was attained in the simulation.

An optimization routine was then used to determine the optimal spacing of the accelerometers. The objective function used in the optimization routine was the squared average difference between $WSSG_{FD}$ and $WSSG_A$ across the face of the entire plate, shown in Eq. (11),

$$\text{Squared Average Diff} = \text{mean}(WSSG_{FD} - WSSG_A)^2. \tag{11}$$

This routine was repeated for each frequency of interest to see how the optimum changes with frequency. It is important to note that the optimal spacing for the accelerometers is highly dependent upon the individual accelerometers and system used. Some systems may have more random noise than others, and so, a new optimization routine should be run each time a system is changed.

It was discovered that the optimal spacing for the accelerometers is dependent upon the frequency of the excitation force and the resonance frequencies of the plate. When the plate was excited at a low frequency, away from the resonance frequencies, the plate did not vibrate with very large amplitudes. This meant that two closely spaced accelerometers were reading nearly the same value, and so any random noise in the system had a great effect on the calculation of WSSG. The accelerometers needed to be spread farther apart in order for them to read significantly different values. Conversely, when a resonance frequency was approached, the plate vibrated with larger amplitudes and so two closely spaced accelerometers did read significantly different values. This caused $WSSG_{FD}$ to be closer in value to $WSSG_A$ and the accelerometers could be placed closer together before random noise became a significant factor.

This means there is not a single spacing which will give the optimal WSSG performance for all frequencies. If only one frequency is to be attenuated, then an optimal spacing can be calculated. If a range of frequencies is to be attenuated, then an average must be made over the range of interest. This is what was done for the experimental tests shown in this paper. It was determined that the optimal spacing for the accelerometers based on the expected noise levels in the authors' experimental setup was approximately 0.0243 m. This value is close to the standard English inch (0.0254 m) and so a value of 0.0254 m was chosen as the spacing to be used in all experimental tests.

In addition to noise and finite difference errors in the calculation of WSSG, the authors also explored the possibility that phase and amplitude differences between individual accelerometers could cause errors in the experimental measurements. The phase and amplitude differences between the accelerometers were tested by placing all four accelerometers on a flat, stiff shaker and recording a signal from all accelerometers using a Bruel and Kjaer Pulse signal analyzer. It was determined that the differences between the amplitudes of the accelerometers were approximately one order of magnitude below the amplitude of the estimated random noise in the experimental setup. This means the random measurement noise has a much greater impact on the accuracy of WSSG than amplitude differences in the accelerometers. The difference in the phases of the accelerometers was also determined to be negligible. It was thus determined that four accelerometers placed in the configuration shown in Fig. 2 was a viable option for measuring WSSG experimentally.

C. Degenerate modes

During experimental tests using a scanning laser Doppler vibrometer (SLDV), it was determined that there are cases when two structural mode shapes occur at nearly the same frequency. These are called degenerate modes. Common sources of degenerate modes are plates whose x and y dimensions are integer multiples of each other. Because the frequencies of these two modes are so close to each other, the two individual mode shapes will superimpose on top of each other and cause distortions in the resulting structural response. This distorted mode shape is often quite different in appearance from normal modes. It was discovered during experimental tests that the WSSG-based control method often did not achieve significant sound attenuation of degenerate modes and it became necessary to perform more simulations to understand the phenomenon.

New simulations were created which calculated the velocities of a simply supported plate whose length was equal to the width of the plate. Sound power levels were calculated using the method of elementary radiators[9] when the plate was being excited with a single point force and then compared to sound power levels when WSSG was being minimized at a single point by a control force. These plots demonstrated that the performance of WSSG as a sound power minimization parameter suffered whenever a degenerate mode was present. Often, little or no attenuation was achieved and even when attenuation was achieved, it was not as effective as non-degenerate modes. An example of one of these plots is shown in Fig. 3. In this figure, the degenerate modes are located at 19, 38, 49, and 64 Hz.

It was determined that degenerate modes simulate an additional degree of freedom of motion to the plate. Thus, there were two degrees of motion, but only one degree of control. It was theorized that adding a second degree of control to the plate would increase attenuation results by allowing the control algorithm to account for both degrees of motion. This hypothesis was tested by adding a second control force to the plate and coding the simulations to minimize WSSG by controlling both control forces simultaneously. Figure 4 shows the sound power radiated when two shakers are used to control the simply supported plate.

This figure shows that adding a second control force does allow WSSG to effectively control the plate when degenerate modes are present. The degenerate modes at 19 and 64 Hz

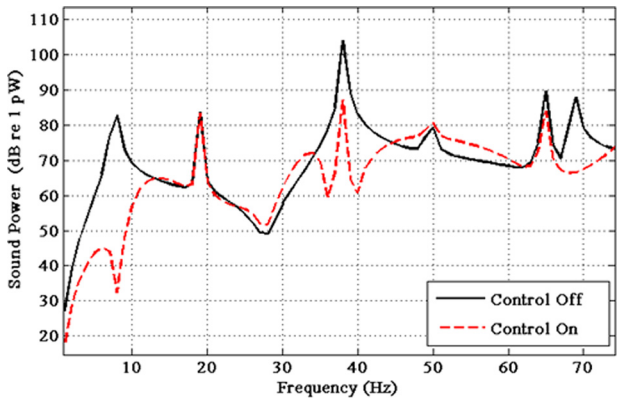

FIG. 3. (Color online) Simulated sound power radiated with a single control force for a plate with degenerate modes.

were attenuated significantly. The (2, 3) and (3, 2) modes located at 49 Hz were not attenuated significantly, but it did perform better than it did when only one control force was present. When one control force was present, WSSG amplified the sound power at that location, but when two were present, it brought the peak down to the level of the surrounding frequencies. Results similar to this were observed for several different control and plate configurations. This led the researchers to believe that controlling a degenerate mode is possible if an additional control force is added.

IV. EXPERIMENTAL RESULTS

This section details the experimental work using WSSG as the minimization quantity in the acoustic control of a vibrating simply supported plate. The setup of the experiment is shown, followed by plots of WSSG as measured across the surface of the plate for several modes. This was done to validate the uniformity of WSSG and to ensure it matches the theory developed by Fisher *et al.*[8] Control plots are then shown for both one and two control force situations and these are compared to the computer simulations with the same configurations. The results are then presented and discussed.

A. Setup

A simply supported plate was assembled using 6061-T6 rolled aluminum; a list of the properties is given in Table I.

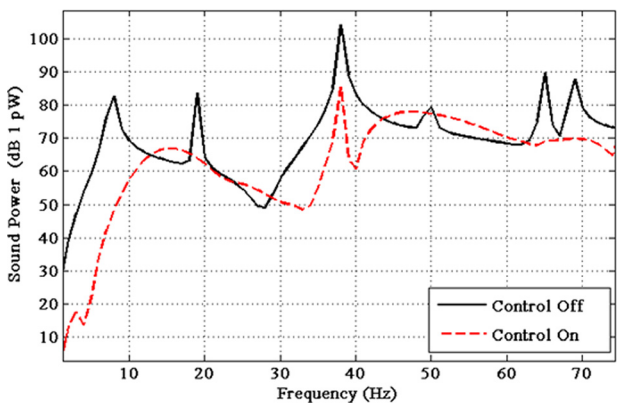

FIG. 4. (Color online) Simulated sound power radiated with two control forces for a plate with degenerate modes.

TABLE I. Properties of the simply supported plate.

Property	Value
Length (x direction) (L_x)	0.4731 m
Length (y direction) (L_y)	0.7525 m
Thickness (h)	0.0032 m
Young's modulus (E)	68.9 GPa
Poisson's ratio (ν)	0.334
Density (ρ)	2700 kg/m^3
Damping ratio (η)	2%

The simply supported boundary conditions were created by suspending the plate in a stiff frame with set screws, spaced 1.6 cm apart, whose points touch the four sides of the plate as shown in Fig. 5. Spatially dense velocity measurements across the entire plate were made with an SLDV to ensure the simply supported boundary conditions were met.

The plate was excited with a Labworks ET-126 shaker attached to a signal generator and controlled with a Bruel and Kjaer type 4809 Vibration Exciter. These shakers were suspended from a stiff frame and attached to the plate by gluing the individual stingers to the back side of the plate. WSSG was measured at a point using four accelerometers placed 0.0254 m apart in the configuration shown in Fig. 2. The accelerometer signals were passed through a filter and into a digital signal processor (DSP) controller which calculated WSSG using Eqs. (7)–(10). Control was achieved using a modified filtered-X LMS algorithm in the DSP controller which optimized the phase and amplitude of the control shaker to minimize WSSG. The specifics of the changes made to the Filtered-X LMS algorithm are given by Fisher.[13] For this work, the reference signal was readily available from the signal generator used to excite the primary shaker, but if this is not available in practice, other techniques can be used to obtain a suitable reference signal from an accelerometer on the plate or from a microphone in close proximity.[14] The SLDV was used to measure the velocity at an array of points on the plate and then sound power was calculated using the method of elementary radiators.[9] A schematic of the experimental setup is shown in Fig. 6.

The simply supported plate was then placed in a window between two large acoustic reverberation chambers. This

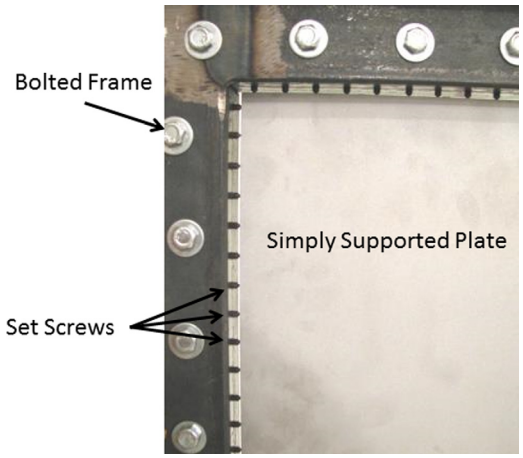

FIG. 5. (Color online) The simply supported boundary conditions.

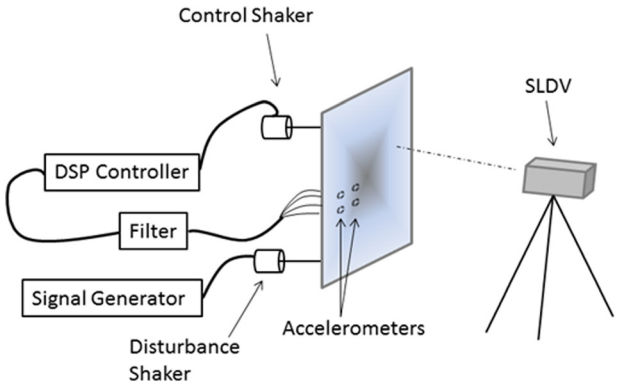

FIG. 6. (Color online) Schematic of the experimental setup.

provided a baffle between the two sides of the plate and isolated the plate from any outside vibrations or noises. The two reverberation chambers had dimensions of $4.96\,\text{m} \times 5.89\,\text{m} \times 6.98\,\text{m}$ and $5.70\,\text{m} \times 2.50\,\text{m} \times 4.30\,\text{m}$. These chambers had multiple axial, tangential and oblique room modes whose resonances fell within the frequency range of the WSSG tests, and so it is possible these could have caused additional loading on the plate. No attempt to analyze the room mode effects on the vibrating plate was made in this paper.

B. Experimental validation of WSSG

Before the plate was set up in the manner shown in Fig. 6, it was necessary to validate the uniformity of WSSG and ensure that it matched theory. This was done by placing a single shaker in the lower right corner of the plate and measuring WSSG across the face of the plate for several of the modes. Only one lightweight shaker was used in order to cause the least amount of distortion in the structural modes. The four WSSG terms were calculated by applying Eqs. (7)–(10) to the SLDV measurements. The individual WSSG terms are shown in Fig. 7.

These four terms match the analytical plots given in the paper by Fisher *et al.*[8] When these four modes are combined using the proper weights, a nearly uniform quantity is obtained. Figure 8 shows the combined WSSG field for the first mode. This is a close match to the analytical plots but it is not perfect. The higher values at the lower part of the plate are due to the placement of the shaker at the bottom of the plate. This caused the first structural mode to skew slightly downward and higher derivatives were measured at the lower portion of the plate, as evidenced by the $(\partial w/\partial y)^2$ plot in Fig. 7.

Figure 9 shows plots of the combined WSSG fields for the next four modes when the ideal mode-specific weights are used. These plots show that experimentally measured WSSG may not be perfectly uniform for higher modes. The non-uniformities on each of these plots can be traced to the non-uniform amplitudes of the individual anti-nodes in each mode shape. For example, on the fourth mode [the (2, 2) mode], the shaker is located in the lower right corner of the plate, much closer to the lower right anti-node than the lower left. The SLDV scans showed that this caused the right anti-node to have a higher amplitude than the left anti-node. Perfect uniformity was thus not obtained. However, the amplitude of the left anti-node is still approximately 90% of the amplitude of the right anti-node, and so, minimizing WSSG in either quadrant should cause similar effects to the sound field.

Modes three and five both had larger variations in the amplitudes of each anti-node and so were not very uniform. This is because the third mode is actually a degenerate mode with the (2, 1) mode and the (1, 3) modes superimposing on each other. Mode five is close to being degenerate, and its

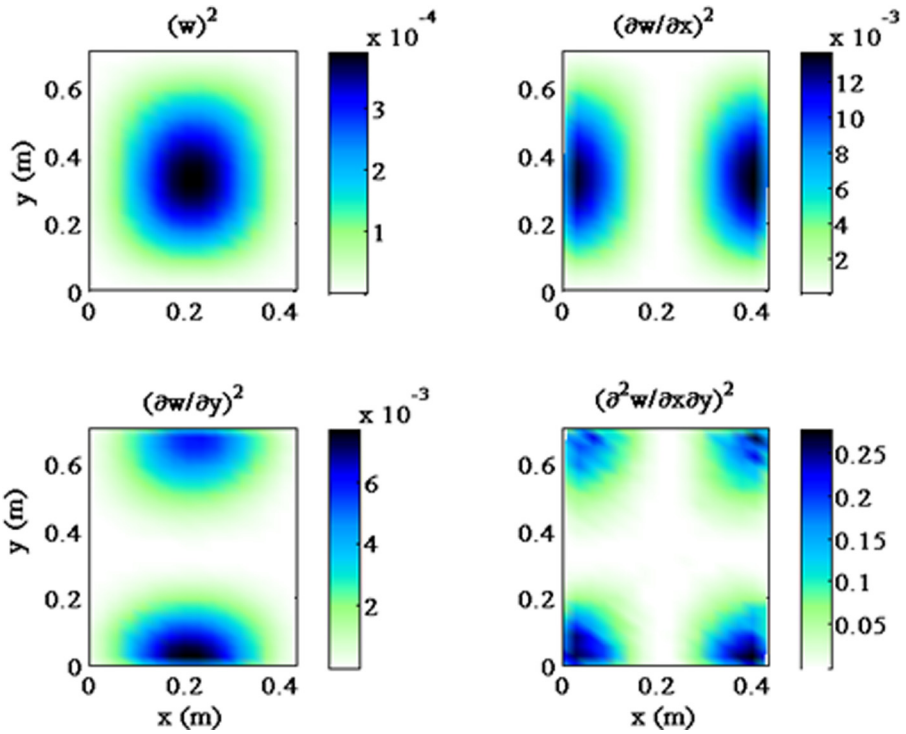

FIG. 7. (Color online) Plots of the four WSSG terms the first mode.

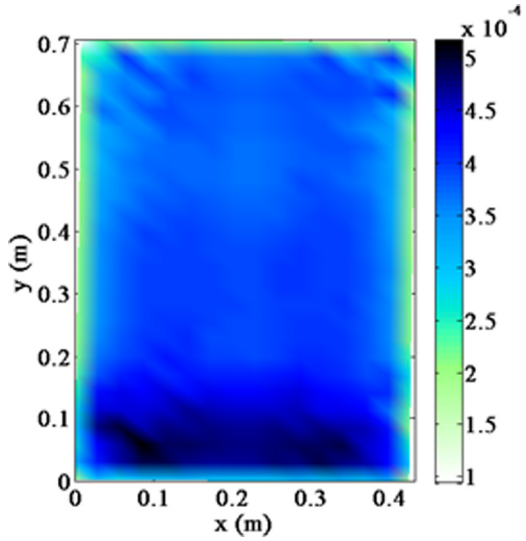

FIG. 8. (Color online) Total WSSG field from the first mode, with frequency specific weights.

(1, 4) mode is greatly influenced by the nearby (2, 3) mode. Similar results were noticed for higher modes. Whenever a resonance frequency was isolated (far away from any other resonance frequency) a nearly uniform WSSG field was calculated, but when natural frequencies were close to each other, then the WSSG field was less uniform.

Some of these non-uniform effects had been predicted by the computer simulations when natural frequencies were closely spaced, but the experimental results showed even more pronounced amplitude differences.

C. Experimentally measured sound power results

The plate was set up in its first configuration and the computer model updated so that the sensor and shaker positions would match the experimental configuration. This allowed for a comparison between analytical models and experimental data. Several configurations were tested, each with different sensor and shaker positions. However, only

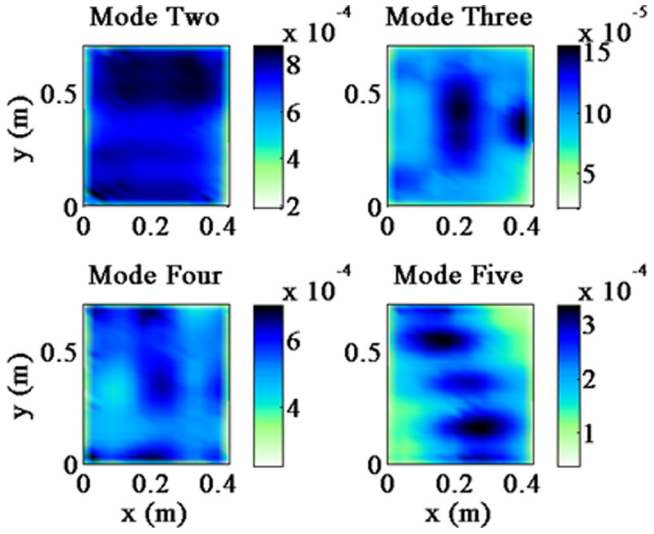

FIG. 9. (Color online) Plots of WSSG for modes two through five.

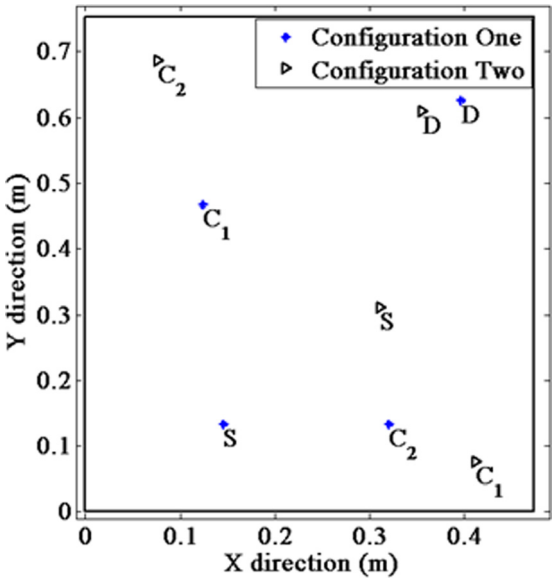

FIG. 10. (Color online) Experimental simply supported plate configurations. D is the disturbance force location; C_1 is first control shaker location; C_2 is the second control shaker location; and S is the WSSG sensor location.

four tests, representing two different configurations, will be shown in this paper. The shaker and sensor positions for each configuration are shown in Fig. 10, with the locations given in Table II.

It was noted that the two shakers used in the experimental results were relatively heavy (well over 5 kg) and thus provided a source of damping, stiffness, and mass loading to the plate. These heavy shakers were necessary in order to create clean signals at low frequencies. The mass loading and additional stiffness from the shakers were not modeled in the computer simulations but caused the resonance frequencies of the experimental plate to shift, often significantly from the values computed by the model. Therefore, the simulated and experimental results were not plotted on the same graph. However, a comparison can still be made between the results by comparing the frequencies with the same mode shapes. The shakers also changed the damping coefficient of the plate. With the shakers attached to the plate an experimental damping coefficient was measured to be 2% ($\eta = 0.02$) using the method of logarithmic decrement. This is higher than the damping coefficient measured without the shakers attached.

Figures 11 and 12 show the numerical and experimental plots, respectively, for configuration one with a single control force. The analytical models were made with a frequency increment of 1 Hz, while the experimental tests were

TABLE II. Actuator and sensor locations.

Actuator/Sensor	Configuration onelocation (x, y)	Configuration twolocation (x, y)
Disturbance	(0.397, 0.625)	(0.406, 0.686)
Controller one	(0.124, 0.467)	(0.413, 0.076)
Sensor	(0.146, 0.133)	(0.311, 0.311)
Controller two (if applicable)	(0.321, 0.1334)	(0.076, 0.686)

TABLE III. Attenuation levels for one control shaker.

	Configuration One		Configuration Two	
Mode	Simulation (dB)	Experimental (dB)	Simulation (dB)	Experimental (dB)
1-1 Mode	37.9	26.7	36.7	26.6
1-2 Mode	15.6	9.4	19.7	11.8
2-1 Mode	14.4	19.2	26.9	5.3
1-3 Mode	7.2	0.7	30.5	14.8
2-2 Mode	6.8	2.3	7.8	4.0
1-4 Mode	-	-	7.5	3.2
2-3 Mode	-	-	1.5	1.6
Overall attenuation	6.1	1.4	3.3	2.7

made with a frequency increment of 5 Hz. Additional experimental data points were also measured at each of the resonance frequencies in order to accurately measure the peaks.

These plots demonstrate several important features about the use of WSSG in an experimental setup. First is that the experimental plots generally show the same trends and shapes as the computer simulations, but the amplitudes of the attenuations are generally smaller. Table III contains the attenuation levels for each mode, as well as the overall sound power attenuation. This table shows that both plots have significant attenuation levels at the (1, 1) mode, (1, 2) mode and (2, 1) mode, with smaller attenuation levels at the (1, 3) and (2, 2) modes. The largest discrepancy between the two plots comes at the (1, 3) and (2, 2) modes, where the computer simulations predict 7.2 and 6.8 dB of attenuation, respectively, but the experimental tests attain only 0.7 and 2.3 dB of attenuation, respectively.

Figures 11 and 12 both show an amplification of radiated sound power in between the (1, 2) and (2, 1) modes. The maximum amplification levels for the simulated and experimental plots are 7.8 and 9.8 dB, respectively. While this may appear to be a large level of amplification, these amplifications occur in between modes, where the uncontrolled power levels are much lower. Thus the amplified levels are still 15 to 20 dB below the levels radiated by the resonance frequencies. These amplified levels have little effect on the overall attenuation levels attained.

The computer simulations predict an overall attenuation of 6.1 dB, while the experimental plots show an overall attenuation of only 1.4 dB. The low overall attenuation of the experimental data is chiefly due to the fact that the experimental results show very minimal sound attenuation for the (1, 3) mode, which has the highest sound power level. Significant control is achieved elsewhere, but the mode which outputs the most sound power is not well controlled.

If the total sound power levels are calculated for just the first three modes (from 35 to 130 Hz) then 6.2 dB of attenuation is achieved in the experimental results. This represents a significant reduction in sound power levels over that frequency range.

One of the main reasons for the attenuation amplitude level differences between the computer models and the experimental plots may be noise. It was demonstrated in Sec. III B that an optimal accelerometer spacing can be found to minimize the effects of noise in the system, but not to eliminate the effects completely. Even with the optimal accelerometer spacing, there was still an 8% to 9% difference between $WSSG_{FD}$ (with noise) and $WSSG_A$ at the resonance frequencies in the computer simulation. These differences were amplified when the plate was being forced at an off resonance frequency and often there was a 20% difference between $WSSG_{FD}$ and $WSSG_A$ in the simulations. Errors in the measured WSSG values make it difficult for the control algorithm to find the optimal values of the amplitude and phase for the control shaker, which will lessen the amount of control achieved. This may account for the amplitude differences between the numerical and experimental sound power plots.

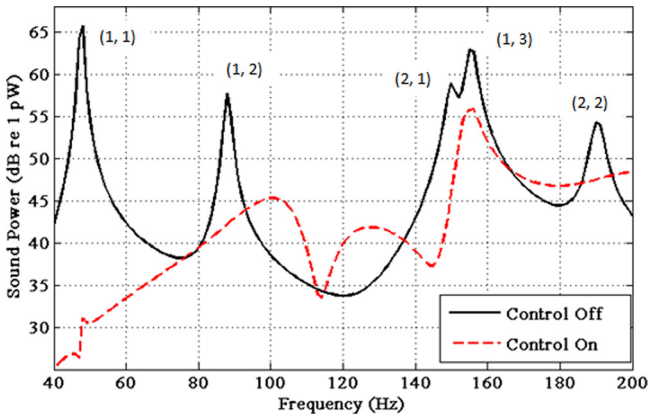

FIG. 11. (Color online) Computer simulation of sound power results for control of WSSG in configuration one with one control force.

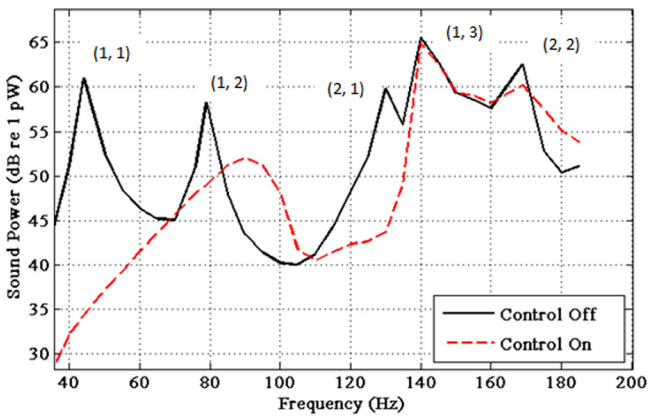

FIG. 12. (Color online) Experimental sound power results for control of WSSG in configuration one with one control force.

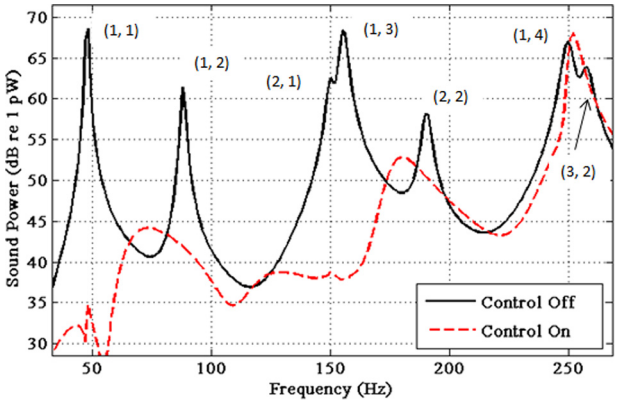

FIG. 13. (Color online) Computer simulation of sound power results for control of WSSG in configuration two with one control force.

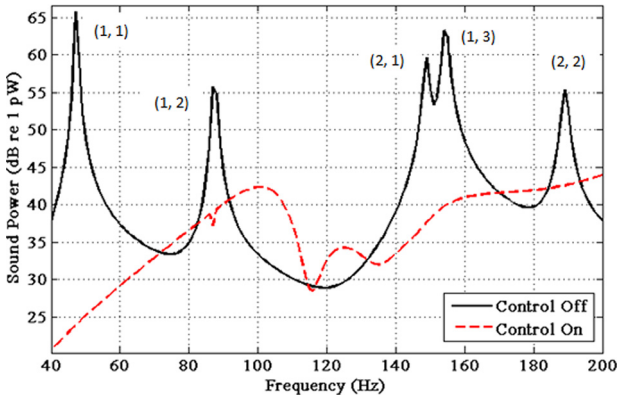

FIG. 15. (Color online) Computer simulation of sound power results for control of WSSG in configuration one with two control forces.

Another possible reason for the differences is that the experimentally measured WSSG was not as uniform across the plate as the theory predicted for higher modes. This was mentioned in Sec. IV B. This means it is possible the accelerometers may not have been located in the best position to measure the vibration of the plate. No attempt was made to optimize the location of the accelerometers on the plate in this paper.

Figures 13 and 14 show the numerical and experimental plots, respectively, for configuration two with one control force and were expanded to include the first seven modes instead of only five. These plots showed similar trends as in configuration one, but with one major difference: the natural frequencies shifted significantly between the (2, 1) and (2, 2) modes on the experimental plots. This frequency shift was shown to be a result of the added mass loading from the shakers. This was shown by measuring the frequency response of the plate twice; once with the heavy disturbance and control shakers attached in configuration two and once with a single (much lighter) LDS V203 shaker placed in the corner. The frequency response of the plate with the lighter LDS shaker closely matched the frequency response of the simulated plate. The frequency response of the plate with the heavy disturbance and control shakers attached showed shifted frequencies. The only difference between the setup of the two measured experimental frequency responses was the shakers attached to the plate. This suggests the shakers were mass loading the plate, which caused the shifted frequencies.

The shifted frequencies of the experimental results make it difficult to do a direct comparison between the simulated and experimental data, but important insights can still be gained. Figures 13 and 14 both show significant attenuation at the first four modes and moderate attenuation at mode five (the (2, 2) mode). Both also show minimal control at the (1, 4) and (3, 2) modes with amplification occurring between their peaks. As was the case in configuration one, the experimental plot showed much lower levels of attenuation, even though the same general trends were seen. Similarly, both plots had some frequencies which were amplified. The simulation predicted an overall attenuation of 3.3 dB attenuation, while the experimental plots showed an actual overall attenuation of 2.7 dB. Both plots achieve attenuation of the major source of radiated power [the (1, 3) mode], but both plots fail to achieve significant control on the sixth and seventh modes [the (1, 4) and (3, 2) modes].

If overall attenuation levels are calculated for just the first five modes (from 50 to 210 Hz) then 6.5 dB of attenuation is achieved on the experimental plate. This is a significant level of attenuation for that frequency range, and

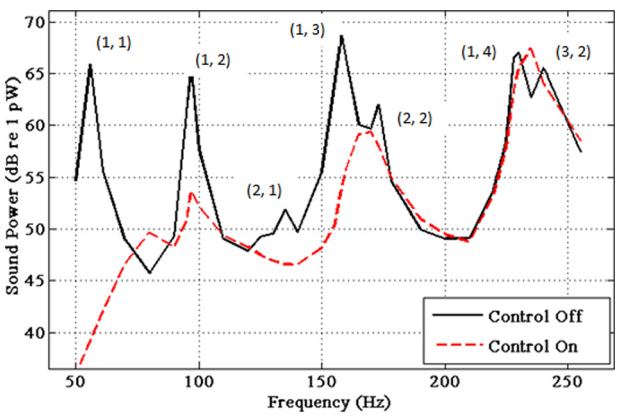

FIG. 14. (Color online) Experimental sound power results for control of WSSG in configuration two with one control force.

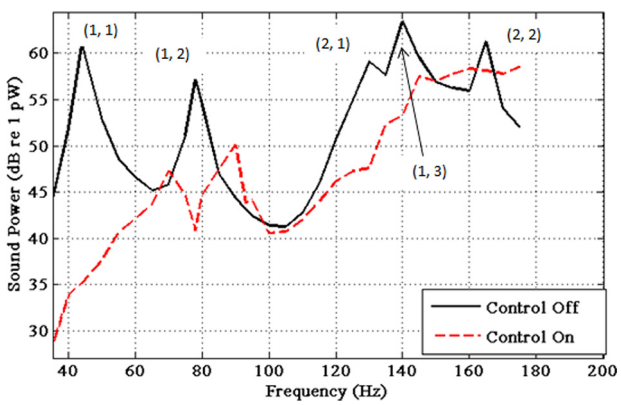

FIG. 16. (Color online) Experimental sound power results for control of WSSG in configuration one with two control forces.

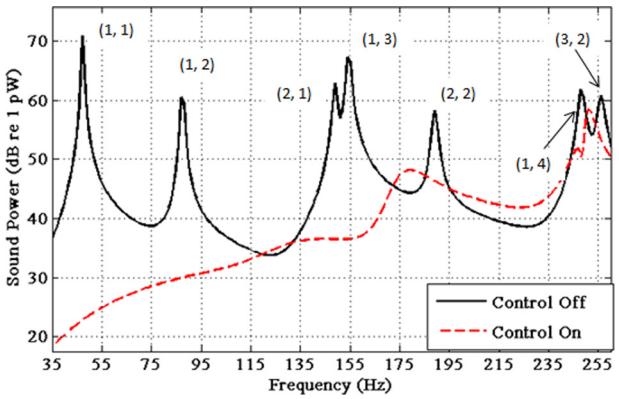

FIG. 17. (Color online) Computer simulation of sound power results for control of WSSG in configuration two with two control forces.

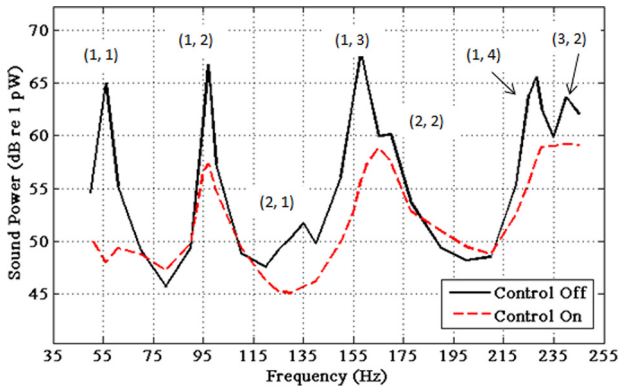

FIG. 18. (Color online) Experimental sound power results for control of WSSG in configuration two with two control forces.

demonstrates that there are situations where WSSG performs very well.

As was noted earlier, several of the resonance frequencies where WSSG fails to cause significant attenuation are close to being degenerate modes. Thus, both tests were performed again with an additional control force added to the plate in order to better control the frequencies near the semi-degenerate modes. The shaker added was an LDS V203 shaker. The results of these tests are shown in Figs. 15–18. Figures 15 and 16 show the numerical and experimental plots, respectively, for configuration one and Figs. 17 and 18 show the numerical and experimental plots, respectively, for configuration two.

These results once again show that the experimental results have the same general shapes and trends as the simulated results, but less attenuation. In configuration one (Figs. 15 and 16), using two control shakers increased the overall attenuation by 5 dB in the simulated results, and by 1.9 dB in the experimental results. This increase was caused mainly by the added control achieved at the (1, 3) mode, which was the largest contributor to total sound power radiated. The list of attenuation levels for each mode is presented in Table IV. The list further confirms the analysis presented in Sec. III C, which showed that adding a second control force significantly helps control degenerate modes.

In configuration two (Figs. 17 and 18), using two control shakers increased the overall attenuation by 5.2 dB in the simulated results and by 2.7 dB in the experimental results. This increase was chiefly due to the additional control attained at the (1, 4) and (3, 2) modes, which had only minimal control with one control force. Adding a second control force does actually increase the number of frequencies which are amplified in configuration two, especially between the (2, 2) and (1, 4) modes, but these frequencies are still 15 dB below the highest sound power levels on the plots. Thus, they do not cause a significant overall amplification.

Similar results were seen in the additional configurations tested, but they were not shown in this paper. In these configurations adding a second control force amplified some of the frequencies between modes, but attenuated the peaks better than a single control force. This shows that adding a second control force to the WSSG method of controlling a radiating simply supported plate may make the method more effective, and should be done where possible. The authors felt that adding a second control force can be implemented on most structures without significantly increasing the setup time or complexity of the process.

Additionally, it was noted that the best control results were attained when the control shakers were located near the edges, and the WSSG sensor located near the center of the plate. Placing the shakers near the edges minimizes the mass loading and stiffness effects of the shakers, which causes fewer distortions in the WSSG field.

V. CONCLUSIONS

The results shown in this paper demonstrate that WSSG can be used to attenuate noise from a vibrating rectangular simply supported plate. Preliminary investigations also show that

TABLE IV. Attenuation levels for two control shakers.

	Configuration One		Configuration Two	
Mode	Simulation (dB)	Experimental (dB)	Simulation (dB)	Experimental (dB)
1-1 Mode	41.9	25.7	48.2	17.1
1-2 Mode	16.8	16.3	30.6	9.4
2-1 Mode	21.9	11.5	26.5	5.9
1-3 Mode	26.5	10.1	30.7	12.2
2-2 Mode	12.8	3.1	12.0	2.6
1-4 Mode	-	-	11.4	8.2
2-3 Mode	-	-	7.3	4.5
Overall attenuation	11.1	3.3	8.4	5.3

the WSSG technique can be applied to structures with other boundary conditions and significant control can be achieved. The WSSG terms have been shown to be relatively uniform on flat plates independent of the boundary conditions. Future work will consist of investigating other boundary conditions and other geometries such as ribbed plates and cylinders.

Attenuation in the simply supported plate is achieved by minimizing WSSG at a single point on the plate through optimizing the amplitude and phase of a single control force. This attenuation can be increased by adding a second control force and keeping just the one WSSG sensor. The addition of the second control force helps attenuate noise coming from degenerate modes.

There were a few differences between the WSSG theory and the experimental data, two of which were the non-uniformity of WSSG for higher-order modes and smaller levels of attenuation achieved than predicted. The theory of WSSG predicted that WSSG would be uniform across the face of the plate for individual modes. This did not completely hold for higher modes. Higher modes often did not have uniform values due to the superposition of degenerate modes.

The overall attenuation measured in the experimental results was less than the models predicted in every case. This was likely due to noise in the measurement of WSSG. The noise levels were such that a 10% to 20% difference was observed between the predicted WSSG values and the measured values. This limited the ability of the control algorithm to minimize WSSG and thus the ability to attenuate the noise emissions.

Despite these differences, significant control was still achieved. When two shakers were used, there was an overall attenuation of 3.3 dB for the first configuration and 5.3 dB for the second configuration. This represents a significant decrease in overall sound power levels. Thus, WSSG should be considered as a viable alternative for use as a minimization quantity in active structural acoustic control of a rectangular simply supported plate. The ease of implementation and relatively unobtrusive nature of the sensors and actuators makes it more practical to use than most other minimization quantities.

Although this paper has focused on simply supported rectangular plates, preliminary results indicate that significant control can be obtained for non-simply supported and non-rectangular plates. It may require more error sensors and control actuators in some cases, but control is expected because the minimization parameter (WSSG) is not a function of boundary conditions or tied to assumptions for rectangular plates. The implementation of the WSSG technique in these cases would be the same as for simply supported rectangular plates which consists of identifying practical locations for the error sensor(s) and control actuator(s). The verification of this process will be explored in future research.

ACKNOWLEDGMENT

This work has been supported by the National Science Foundation Grant NSF CMMI-1130482.

[1]S. D. Snyder and N. Tanaka, "On feed-forward active control of sound and vibration using vibration error signals," J. Acoust. Soc. Am. **94**, 2181–2193 (1993).
[2]S. D. Snyder and C. H. Hansen, "Mechanisms of active control by vibration sources," J. Sound Vib. **147**, 519–525 (1991).
[3]T. C. Sors and S. J. Elliott, "Volume velocity estimation with accelerometer arrays for active structural acoustic control," J. Sound Vib. **258**, 867–883 (2002).
[4]M. E. Johnson and S. J. Elliott, "Active control of sound radiation using volume velocity cancellation," J. Acoust. Soc. Am. **98**, 2174–2186 (1995).
[5]M. E. Johnson and S. J. Elliott, "Volume velocity sensors for active control," Proc. Inst. Acoust. **15**, 411–420 (1993).
[6]J. Pan, S. Snyder, and C. J. Hansen, "Active control of far-field sound radiated by a rectangular panel-A general analysis," J. Acoust. Soc. Am. **91**, 1992–2056 (1991).
[7]C. R. Fuller, "Active control of sound transmission/radiation from elastic plates by vibration inputs: I. Analysis," J. Sound Vib. **136** 1–15 (1990).
[8]J. M. Fisher, J. D. Blotter, S. D. Sommerfeldt, and K. L. Gee, "Development of a pseudo-uniform structural quantity for use in active structural acoustic control of simply supported plates: An analytical comparison," J Acoust. Soc. Am. **131**, 3833–3840 (2012).
[9]F. Fahy and P. Gardonio, *Sound and Structural Vibration: Radiation, Transmission and Response* (Elsevier, Oxford, UK, 2007), pp. 165–175.
[10]G. Pavic, "Measurement of vibrations by strain gauges, Part II: Selection of measurement parameters," J. Sound Vib. **102**, 165–188 (1985).
[11]B. L. Scott and S. D. Sommerfeldt, "Estimating acoustic radiation from a Bernoulli-Euler beam using shaped polyvinylidene fluoride film," J. Acoust. Soc. Am. **101**, 3475–3485 (1997).
[12]S. C. Chapra and R. P. Canale, *Numerical Methods for Engineers*, 5th ed. (McGraw-Hill, New York, 2006), pp. 85–90.
[13]J. M. Fisher, "Development of a pseudo-uniform structural velocity metric for use in active structural acoustic control," M.S. thesis, Brigham Young University, Provo, Utah, 2010.
[14]S. M. Kuo and D. R. Morgan, *Active Noise Control Systems* (John Wiley and Sons, New York, 1996), pp. 82–85.